濟州大學校 産業技術硏究所 論文集, 第9卷, 2號, pp.93-103, 1998. 12
Cheju National Univ. R.I.I.T. Jour., Vol.9, No.2 pp.93-103, 1998. 12

Computer Simulation of Anisotropic Turbulent Flows in Nuclear Subchannels

Hyu-Chan Kim* and Sin Kim**

원자로 부수로를 지나는 비등방성 난류 유동에 대한 전산 실험

김 휴 찬* · 김 신**

ABSTRACT

The prediction of thermal hydraulic field in nuclear subchannels is important to the design and the safety analysis of nuclear reactor. The accurate prediction requires the detailed knowledge of the flow structure, which is complicate due to anisotropic turbulent phenomenon. The flow pulsation phenomenon in rod bundle flow fields has been proposed as one of main causes of anisotropic eddy diffusion. In this study, the anisotropy factor for the fluid flows through rod bundles is estimated with the scale analysis on the flow pulsation phenomenon. Based upon the assumption that the transport process is composed of isotropic turbulent motion (turbulent motion without the flow pulsation) and flow pulsation, the scale relation for the anisotropy factor is derived. The derived scale relation is compared with published experimental results and show good agreements. Also, an anisotropy factor model for the numerical calculation of the turbulent flow field in rod bundles is suggested based on the derived anisotropy factor scale relation.

Key words : Anisotropy factor, Flow pulsation, Scale analysis, Nuclear subchannel

I. Introduction

Nuclear fuel assemblies are comprised of many subchannels, typically rod bundles. The rod bundle flow fields are characterized by secondary flows and strong anisotropy of turbulent diffusivities which are not observed in a circular tube or between parallel plates. Therefore, it is necessary to understand the fundamental characteristics and to predict their effects for the thermal hydraulic analysis of rod bundles.

The experimental results of eddy viscosity in rod

* 제주한라대학 사무자동화과
Dept. of Office Automation, Cheju Halla College
** 제주대학교 에너지공학과
Dept. of Nuclear and Energy Eng., Cheju Nat'l Univ.

bundle geometries show consistency. The normal eddy viscosity is similar to that of the circular tube near the wall and is twice as much far from the wall[1)-3)]. However, the parallel eddy viscosity is quite different from the normal viscosity as well as that of the tube.[1),2)]

Rowe et al.[4)] carried out an experiment on the turbulent mixing phenomenon between subchannels of rod bundles and found a macroscopic flow near the gap. They interpreted it as the cause of the anisotropy.

Bartzis and Todreas[5)] experimentally and numerically investigated the turbulent flow field in triangular-arrayed rod bundles with $P/D=1.124$. They adopted the 2-equation model with anisotropy and secondary flow models and developed a simple anisotropic model for length scales. Their results showed that the effect of anisotropy was greater than that of the secondary flow.

From experiments and numerical analysis, Seale[6),7)] concluded that secondary flow hardly contributed to the velocity and temperature profiles and the high mixing rate at the gap could be modelled with anisotropy. In terms of gap Stanton number, St_g, the isotropic model with secondary flow produced about 13% higher mixing rates than without. However, the discrepancy with the measured data was still very wide up to 10 times. Hence, he decided to include the anisotropic model. He assumed that the anisotropic factor, n, was a function of wall distance because n had the maximum value near the wall and rapidly decreased to about 1. Through testing various functions, he chose the following distribution function:

$$n = 50 \exp\{-(3y/\hat{y})^2\} + 2 . \qquad (1)$$

The calculated St_g with this function agreed with the experimental results within a 50% error.

Slagter[8)] proposed a one-equation model excluding the wall function and analyzed the turbulent flow in rod bundles neglecting the secondary flow. In this work, he used Carajilescov and Todreas' anisotropic length scale model[9)] in order to reflect the anisotropic eddy diffusion. Also, he added some modification to it for the damping effect near the wall.

Yang and Chieng[10)] recommended the following anisotropic factor which had been tested by Seale,[7)]

$$n = 30 \exp\{-(3y/\hat{y})^2\} + 1 , \qquad (2)$$

after they computed the flow and temperature fields with various types of functions neglecting secondary flow.

Wu[11)] analyzed the turbulent flow in a trapezoidal duct with a single rod, and adopted the anisotropy and secondary flow models simultaneously. The Launder-Ying model[12)] was used as an algebraic stress model and the anisotropic factor was developed from the experimental data.

Recently, using scale analysis methodology, Kim and Park[13)] derived scale relations for anisotropy factor and turbulent mixing rate based on the flow pulsation phenomenon under the assumption that the phenomenon might considerably affect the anisotropic feature of eddy diffusion as well as the turbulent mixing in rod bundles. Although their work was a novel attempt, it has proven that their scale relation can not reproduce some experimental data which were not quoted in their work. Hence, in this study, their model should be throughly examined and re-evaluated so as to be modified and extended.

The anisotropy factor is re-estimated with Kim and Park's analysis methodology.[13)] The improved scale relation is compared with experimental data and shows good agreements both with respect to trend and magnitude for various geometries.

Also, an anisotropy factor model for the numerical calculation of the turbulent flow field in

rod bundles is proposed, and the model is verified by comparing the numerical results with experimental data.

II. Flow Pulsation Phenomenon

In compound flow fields connected narrow passages such as rod bundles, macroscopic flow pulsations are observed. Recently, it was reported that this phenomenon could be found even in the gaps between axial fins.[14),15)] Such large scale eddies due to flow pulsation are regarded as the main cause for turbulent mixing since these move across the gap between subchannels and blend the mass, momentum and energy. Since this phenomenon becomes more energetic as the relative gap size is reduced, it can explain why high mixing rates are obtained even in closely packed rod arrays. Also, the flow pulsation may significantly affect turbulent structures such as strong anisotropy of turbulent diffusion as well as mixing.[13)]

Kim and Park[13)] carried out scale analysis on the phenomenon and estimated two main turbulent parameters: anisotropy factor and turbulent mixing rate. These two parameters in rod bundles are essential in precise thermal hydraulic analysis of fuel assemblies by using the distributed and the lumped parameter approaches, respectively. In this work, their model is discussed for the modification of the anisotropic factor scale relation.

2.1. Hypothetical flow

The velocity fluctuation behavior in the gap region should be determined by the interaction with adjacent subchannels rather than being described independently. Experiments show that in rod bundles there are pressure fluctuations acting alternatingly, that is, at one time from right to left and at another time reversely. These make almost periodic

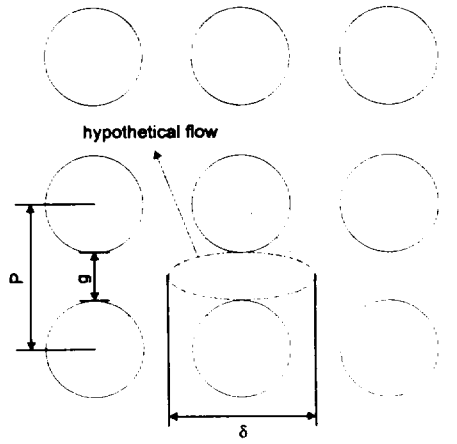

(a) Square array

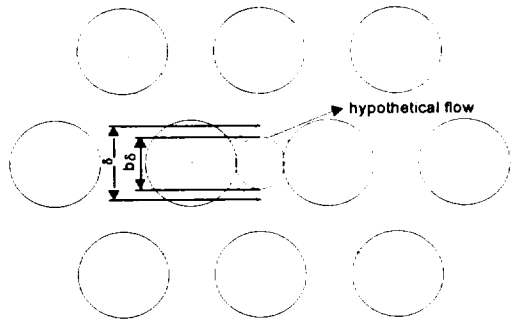

(b) Triangular array

Fig. 1 Schematic of rod bundle geometries

flow pulsations. In order to simulate the flow pulsation, Kim and Park[13)] suggested hypothetical macroscopic flows which move through the gap to the center region of the subchannel circulating clockwise and counter-clockwise alternately between adjacent subchannels. The ellipse in Fig. 1 denotes the hypothetical flow path assumed in this study. These flows are presumed to have the following characteristics:

(1) The flow path is an ellipse whose major and minor axes are half of the parallel and normal length scales of the flow pulsation, respectively.

(2) When the flow pulsation moves from left to

right, the flow circulates clockwise in the upper gap region and counterclockwise in the lower, and vice versa. That is, the two independent flows move in the opposite direction.

(3) The velocity of the flow is equal to that of the flow pulsation at the gap.

(4) The flow circulates with the frequency of the flow pulsation.

2.2. Estimation of the length and velocity scales of the flow pulsation

The spatial correlation coefficient is a measure for the degree of correlation between the variables observed at two spatial points. The experimental results of Hooper and Rehme[16] for the spatial correlation coefficient of the parallel components of the velocity fluctuation showed a value above 0.2. Thus the gap size, g, may be proper for the normal length scale of the flow pulsation, L_y. It was reported that the spatial correlation coefficients between the gap center and the other point were measured above 0.1, even in the central region of the subchannel.[17] Hence, the parallel length scale of the flow pulsation, L_x, is about the centroid-to-centroid distance, δ. Then, Kim and Park[13] suggested that the parallel length scale should be shortened in the triangular-arrayed rod bundle (Type 'T') or at the rod-rod gap of the wall-bounded subchannel (Type 'RR'), since there are obstacles in the front of the flow pulsation. This is different from in the square-arrayed rod bundle (Type 'S') or the rod-wall gap of wall-bounded subchannel (Type 'RW'). They introduced the shape factor b to reflect such openness as:

$$L_x = b\delta\,, \quad L_y = g\,. \tag{3}$$

In this, for an open path such as in the Types 'S' and 'RW', they recommended $b = 1.0$, and for a blocked path such as in Types 'T' and 'RR', $b = 2/3$. In fact, the flow pulsation phenomenon is a pulsation alternating the flow direction. Hence, in this study, it is assumed that in case the configuration of the flow domain permits all of the pulsation to proceed without any interference each other the shape factor is set to be $b = 1.0$. But, if the configuration hinders the pulsations by making neighbouring pulsations collide each other the shape factor should be less than 1 and in this case $b = 2/3$ is assumed. As shown in Fig. 2, square-arrayed rod bundles and wall bounded rod bundles correspond to the first case and triangular-arrayed rod bundles are the second case.

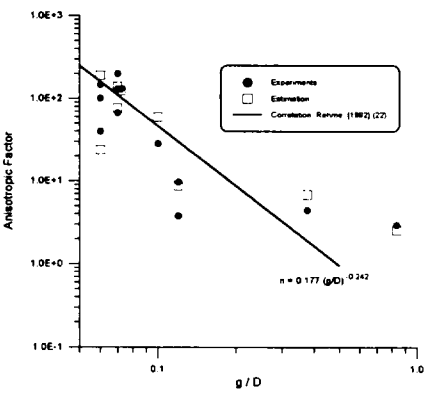

Fig. 2 Experimental and estimated anisotropy factors

The principal frequency of the flow pulsation at the gap f_p can be expressed in terms of the path length z_{FP} and the flow pulsation velocity U_{FP} as $f_p = U_{FP}/z_{FP}$. Hence, introducing Strouhal number $Str = f_p D/u^*$, the parallel and normal velocity scales of the hypothetical flow U_x and U_y can be obtained as

$$\frac{U_x}{u^*} = a_x \frac{z_{FP}}{D} Str \quad and \quad \frac{U_y}{u^*} = a_y \frac{z_{FP}}{D} Str\,. \tag{4}$$

The velocity coefficients a_x and a_y denote the ratio of each velocity scale to U_{FP}. Also, Wu and Trupp's Strouhal number correlation,[18]

$$Str^{-1} = 0.822\left(\frac{g}{D}\right) + 0.144 , \quad (5)$$

is used as recommended by Kim and Park.[13] Since the hypothetical flow has elliptic motion with the major and minor axes, $L_x/2$ and $L_y/2$, respectively, velocities for each direction can be obtained from the kinetic energy conservation. Assuming that v_x and v_y denote the parallel and normal velocity of the fluid particle moving along the ellipse, the particle satisfies following equations:

$$\frac{x^2}{(L_x/2)^2} + \frac{y^2}{(L_y/2)^2} = 1, \quad (6)$$

$$v_x^2 + v_y^2 = U_{FP}^2 . \quad (7)$$

If the average value of each velocity component can be regarded as directional velocity scales of the flow pulsation, the velocity coefficients become

$$a_x = \overline{\frac{v_x}{U_{FP}}} = \frac{2}{\pi}\sqrt{\frac{1}{1-\lambda^4}}\sin^{-1}\sqrt{1-\lambda^2}$$
$$and \qquad a_y = \overline{\frac{v_y}{U_{FP}}} = \frac{2}{\pi}\sqrt{\frac{\lambda^4}{1-\lambda^4}}\sinh^{-1}\sqrt{\frac{1-\lambda^4}{\lambda^4}} \quad (8)$$

where the aspect ratio $\lambda = L_y/L_x$. If the aspect ratio is sufficiently small, the velocity coefficients become approximately

$$a_x = 1 - \frac{2\lambda^2}{\pi} \qquad and$$
$$a_y = (\ln 2 - 2\ln\lambda)\frac{2\lambda^2}{\pi} . \quad (9)$$

These are applicable to any geometry, while in Kim and Park the velocity coefficients were obtained for a square-arrayed rod bundles and they were used for all geometries. As to the path length, it can be approximated as

$$\frac{z_{FP}}{D} = 2\frac{b\delta}{D}\left[1 + \left(-\frac{1}{2}\ln(\lambda) + \frac{1}{2}\ln(4) - \frac{1}{4}\right)\lambda^2\right] \quad (10)$$

Original Kim and Park' expression, however, shows somewhat large differences from the real elliptic path length for small aspect ratios.

III. Estimation of Anisotropy Factor

In order to estimate the anisotropy factor of the turbulent flow $n = \nu_P/\nu_N$ on the basis of the flow pulsation in rod bundles, it is assumed that the observed eddy viscosity consists of two components: the isotropic eddy viscosity without the flow pulsation ν_T and the flow pulsation eddy viscosity caused by this phenomenon. Then, total eddy viscosities for each direction are given as,

$$\nu_P = \nu_T + \nu_x$$
$$and \qquad \nu_N = \nu_T + \nu_y , \quad (11)$$

where ν_x and ν_y are the parallel and the normal eddy viscosities caused by the flow pulsation. If each eddy viscosity can be regarded as a multiplication of corresponding velocity and length scales as Prandtl suggested in the mixing length hypothesis, each eddy viscosity component can be expressed as,

$$\nu_T = C u^* g , \quad (12)$$

$$\nu_x = C U_x L_x , \qquad \nu_y = C U_y L_y . \quad (13)$$

The proportional coefficient C is assumed to be the

same for all cases. The velocity scale of the isotropic eddy viscosity is selected as the friction velocity u^* since u^* is the most typical velocity scale in turbulent flows. As for the length scale, the gap size g is adopted while Kim and Park[13] suggested the profile length at the gap, $g/2$. However, g seems to be more pertinent because the eddy may extend itself to the maximum size that the geometry permits. Consequently, the representative anisotropy factor $\bar{n}$ can be expressed as the ratio of each scale as.

$$\bar{n} = \frac{1 + a_x b \dfrac{(z_{FP}/D)(\delta/D)}{g/D} Str}{1 + a_y (z_{FP}/D)\, Str} \quad . \quad (14)$$

Actually, the anisotropy factor is a function of position. Hence, when Kim and Park[13] compared the scale relation for anisotropy factor with experimental data, they regarded the anisotropy factor at $y/\hat{y} = 0.3$ as a representative value. Table 1 lists the experimental data and the results from the scale relation for anisotropy factor derived in this study as well as those from Kim and Park. As shown in the table, Kim and Park's scale relation fails to reproduce the Meyer's[20] and Krauss and Meyer's[21] experimental data. Hence, it can be deduced that the predictability of the present scale relation is more preferable compared to Kim and Park's.

Rehme[22] reviewed many experimental data of eddy viscosity parallel to the wall close to the gaps and correlated them as a function of the relative gap size g/D. If it is assumed, as he said, that the reference eddy viscosity scaled by friction velocity

Table 1 Experimental and Estimated anisotropy factors

			Experiment	Estimation	
				Kim and Park[13]	Present
Rehme [1978][1]					
P/D = W/D = 1.07		R-R[a]	67	70	76
		R-W[b]	200	220	140
		R-W	130	220	140
Rehme [1987][2]					
P/D = 1.036	W/D = 1.072	R-W	130	200	120
Seale [1979][6]					
P/D = 1.833	W/D = 1.875	R-R	2.94	2.6	2.6
1.375	1.402	R-R	4.44	7.3	6.9
1.100	1.186	R-R	28.32	53	60
Tahir and Rogers [1986][19]					
△[c]P/D = 1.06		R-R	40	54	24
Meyer [1991][20]					
△P/D = 1.12		R-R	3.8	22	8.8
Krauss and Meyer [1995][21]					
△P/D = 1.12	W/D = 1.06	R-R	9.7	22	8.8
		R-W	150	310	190
		R-W	100	310	190

[a]R-R = rod-rod gap. [b]R-W = rod-wall gap. [c]△ = triangular array.

u^* and profile length $\hat{y}$ is 0.1, the anisotropy factor can be expressed as

$$\bar{n} = 0.177\left(\frac{g}{D}\right)^{-2.42} . \quad (15)$$

Figure 2 shows the Rehme's correlation and the estimated anisotropy factors with the experimental data listed in Table 1. As seen in Fig. 2, the experimental data is scattered even at the same g/D. Therefore, even if Rehme's correlation can predict the overall trend of the anisotropic factor according to g/D, it seems to be inappropriate in reflecting the effect of the detailed configuration on the anisotropy since it is expressed only in terms of g/D. On the contrary, the present scale relation considers the detailed configuration of the flow channel and can predict more reasonably.

Ⅳ. Numerical Modeling of Anisotropy Factor

In the analysis on rod bundle flow fields with a distributed parameter model, usually various anisotropic eddy viscosity models are used since without the models the numerical calculations fail to predict the thermal hydraulic behaviors of the flow fields. For this reason, many models have been proposed. However, most of them were selected after the numerical tests performed with prescribed model functions or were made by data fitting with specific experiments without any universal reasoning.

As discussed above, Seale[7] and Yang and Chieng[10] had tested various types of model functions to simulate the anisotropic feature of eddy diffusion and proposed a error function type model function:

$$n = A\exp\{-(By/\hat{y})^2\} + C . \quad (15)$$

Seale concluded $A=50$, $B=3$, and $C=2$, however Yang and Chieng set A, B, and C to be 30, 3, and 1, respectively. Even though they used different model constants, they agreed that the anisotropy has a maximum value adjacent to the wall and rapidly decreases to near unity and the error function is most appropriate to describe such damping characteristics. A means the magnitude of anisotropy and Seale and Yang and Chieng used constant values irrespective of geometry. However many experiments show that the magnitude of anisotropy depends on the geometry.[22] As to C, describing the anisotropy factor on the maximum velocity line, it might be controversial to determine the value. On the maximum velocity line, although there is no apparent evidence that the anisotropy disappear, the isotropic turbulent diffusion can be regarded as a reasonable assumption since the anisotropy may be weak there, as can be seen in Seale and Yang and Chieng.

In this study, in order to reflect the effect of geometry on the anisotropy the anisotropy factor scale relation derived above is used to find A. If it is assumed that the anisotropy at $y/\hat{y}=0.3$ is a representative value and $B=3$ is proper to describe the damping of the anisotropy, A can be expressed as $\bar{n} = A\exp\{-(3\times0.3)^2\}+1$ or $A = 2.25(\bar{n}-1)$. Hence, the anisotropy factor proposed in this study for the numerical analysis of turbulent flow field in rod bundles becomes

$$n = 2.25(\bar{n}-1)\exp\{-(3y/\hat{y})^2\}+1 \quad (16)$$

with the representative anisotropy factor, Eq. (14).

For the verification of the proposed anisotropy factor model, some numerical analyses are performed using the code developed by Kim and Park[23),24)] and adopting the proposed anisotropy factor model. The code uses Lam and Bremhorst low-Reynolds number $k-\varepsilon$ model[25)] to simulate the rod bundle turbulent flow field up to the wall and is formulated in finite

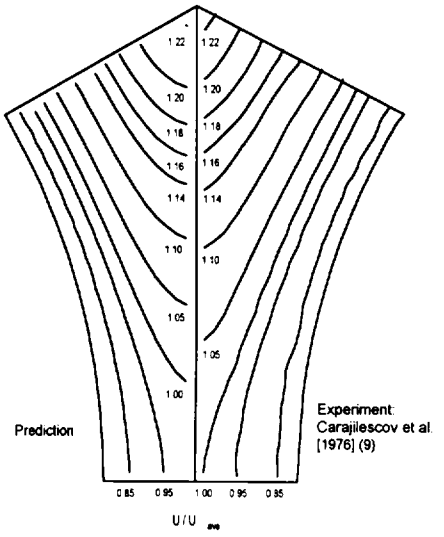

Fig. 3a Axial velocity contour in a triangular array (P/D=1.123, Re=27000)

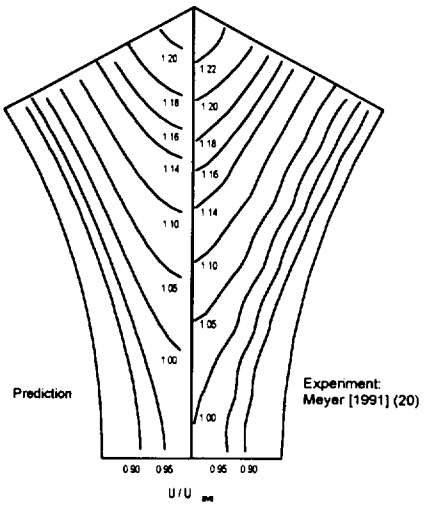

Fig. 3b Axial velocity contour in a triangular array (P/D=1.12, Re=71000)

element method. In order to describe the anisotropic feature of turbulent momentum transport, an anisotropic eddy viscosity model based on Eq. (16) is used. The secondary flow is neglected because it gives only marginal effect on the turbulent flow structure in rod bundles.[7),24)] The full description of the code can be found in Kim and Park's works.[23),24)]

Figure 3 shows the comparison of the computed axial velocity contours with the experimental results on a triangular array of Carajilescov and Todreas[9] for $P/D=1.123$ and $Re=27,000$ and of Meyer[20] for $P/D=1.10$ and $Re=61,000$. The predictions with the present model reproduce the experimental results sufficiently well.

To verify the predictability of wall shear stress, Trupp and Azad's[3] and Meyer's results[20] are compared in Fig. 4. Analogously to the axial velocity profile prediction, the prediction is successful. Especially, Fig. 4b shows the calculated distribution of wall shear stress by Meyer[20] also and the present model produce better agreements. The comparison with the experimental data of Rowe et al.[4] in square-arrayed rod bundles is given in Fig. 5 and it also shows reasonable agreement.

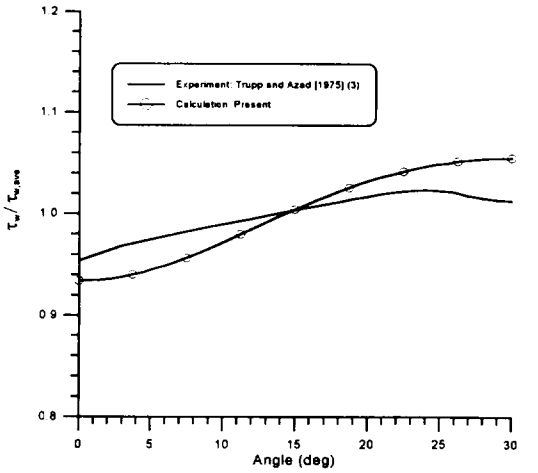

Fig. 4a Wall shear stress variation in a triangular array (P/D=1.20, Re=49000)

V. Conclusions

The flow pulsation phenomenon has been

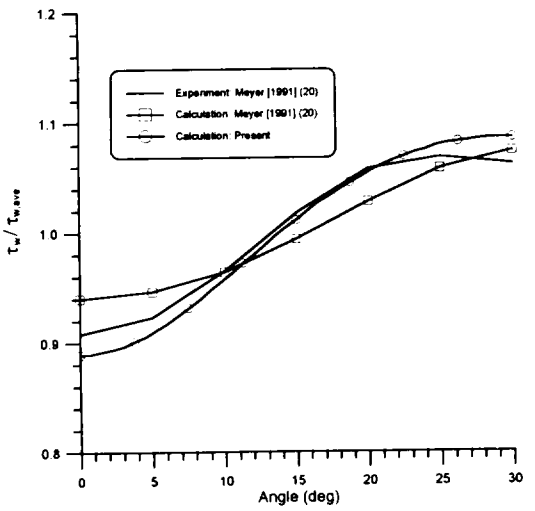

Fig. 4b Wall shear stress variation in a triangular array (P/D=1.12, Re=27000)

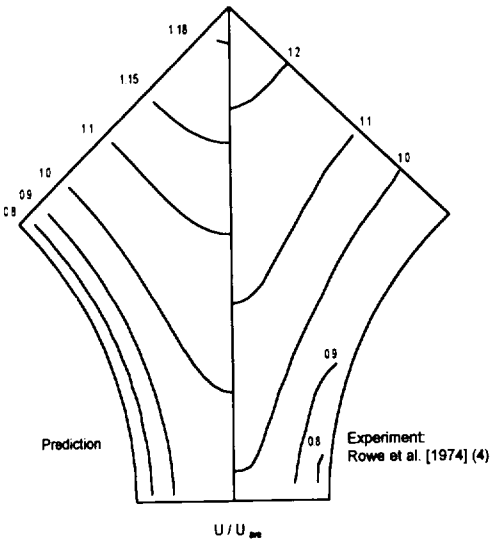

Fig. 5 Axial velocity contours in a square array (P/D=1.25, Re=100,000)

highlighted as a main cause for turbulent mixing. Under the assumption that the flow pulsation also affect the turbulent structure and can be a major contributor to the anisotropy feature of the turbulent diffusion, a scale analysis on the flow pulsation is performed following Kim and Park's attempt[13] to obtain the anisotropy factor. As a result, a new scale relation for anisotropy factor is suggested. The derived scale relation is verified with published experimental data for various geometry. It can be concluded that the flow pulsation is a significant contributor to the anisotropic turbulent diffusion.

Moreover, adopting the derived anisotropy factor scale relation in this study, an anisotropy factor model is developed for numerical analysis on the turbulent flow fields in rod bundles. The numerical results with the model are successfully compared with published experimental data. Therefore, the model will be useful in the thermal hydraulic analysis on the nuclear subchannels comprised of rod bundles.

Nomenclature

a_x, a_y	velocity coefficients
b	shape factor
C	arbitrary proportional coefficient
D	rod diameter
g	gap size
L_x, L_y	length scales of flow pulsation
n	anisotropy factor
$\overline{n}$	representative anisotropy factor at the gap
P	rod pitch
Str	Strouhal number
u^*	friction velocity
U_{FP}	velocity of flow pulsation at the gap
U_x, U_y	velocity scales of flow pulsation
v_x, v_y	parallel and normal velocities of hypothetical circulating flows
W	wall pitch

$\hat{y}$	profile length
z_{FP}	hypothetical path length of flow pulsation

Greek

δ	centroid-to-centroid distance
ν_T	isotropic eddy viscosity
ν_x, ν_y	parallel and normal eddy viscosity due to the flow pulsation, respectively

요 약

원자로 부수로에서의 열수력학적 거동을 예측하는 것은 원자로의 설계나 안전해석에 중요한 일이다. 정확한 예측을 위해서는 유동 구조에 대한 상세한 지식이 필요한데, 유동 구조는 난류의 비등방성 때문에 복잡하다. 봉다발 유동장에서 관찰되는 유동맥동 현상이 비등방성 와류확산의 주요 원인 중 하나로 제안되고 있다. 본 연구에서는, 봉다발을 지나는 유동의 비등방성 인자를 유동맥동에 대한 척도 해석을 통해 평가하였다. 수송 과정이 등방성 난류 운동 (유동맥동이 배제된 난류 운동)과 유동맥동으로 구성되어 있다는 가정 아래, 비등방성 인자에 대한 척도관계식을 유도하였다. 유도된 척도관계식을 기존의 실험자료와 비교하여 잘 일치하고 있음을 알 수 있었다. 또한, 유도된 비등방성 인자 척도관계식을 바탕으로 봉다발 난류 유동장의 수치해석을 위한 비등방성 인자 모델을 제안하였다.

Acknowledgements

The author wishes to acknowledge the financial support of the "Nuclear Academic Research Fund by Korean Ministry of Science & Technology" made in the program year of 1998.

References

1) Rehme, K., 1978, The Structure of Turbulent Flow through a Wall Subchannel of a Rod Bundle," Nucl. Eng. Des., Vol. 45., pp. 311-323.
2) Rehme, K., 1987, The Structure of Turbulent Flow through Rod Bundles, Nucl. Eng. Des., Vol. 99, pp. 141-154.
3) Trupp, A. C. and Azad, R. S., 1975, The Structure of Turbulent Flow in Triangular Array Rod Bundles, Nucl. Eng. Des., Vol. 32., pp. 47-84.
4) Rowe, D. S., Johnson, B. M. and Knudsen, J. G., 1974, Implications Concerning Rod Bundle Crossflow Mixing Based on Measurements of Turbulent Flow Structure, Int. J. Heat Mass Transfer, Vol. 17, pp. 407-419.
5) Bartzis, J. G. and Todreas, N. E., 1979, Turbulence Modeling of Axial Flow in a Bare Rod Bundle, J. Heat Transfer, Vol. 101, pp. 628-634.
6) Seale, W. J., 1979, Turbulent Diffusion of Heat between Connected Flow Passages, Part I: Outline of Problem and Experimental Investigation, Nucl. Eng. Des., Vol. 54., pp. 183-195.
7) Seale, W. J., 1979, Turbulent Diffusion of Heat between Connected Flow Passages, Part II: Predictions Using the 'k-ε' Turbulence Model, Nucl. Eng. Des., Vol. 54., pp. 197-209.
8) Slagter, W., 1982, Finite Element Solution of Axial Turbulent Flow in a Bare Rod Bundle Using One-Equation Turbulence Model, Nucl. Sci. Eng., Vol. 82, pp. 243-259.
9) Carajilescov, P. and Todreas, N. E., 1976, Experimental and Analytical Study of Axial Turbulent Flows in an Interior Subchannel of Bare Rod Bundle, J. Heat Transfer, Vol. 98, pp. 262-268.
10) Yang, A.-C. and Chieng, C.-C., 1987, Turbulent

Heat and Momentum Transports in an Infinite Rod Array, J. Heat Transfer, Vol. 109, pp. 599-605.

11) Wu, X., 1994, Numerical Study on the Turbulence Structures in Closely Spaced Rod Bundle Subchannels, Num. Heat Transfer, Vol. 25, pp. 649-670.

12) Launder, B. E. and Ying, W. M., 1973, Prediction of Flow and Heat Transfer in Ducts Square Cross-section, Proc. Instn Mech. Engrs, Vol. 187, pp. 455-461.

13) Kim, S. and Park, G.-C., 1997, Estimation of Anisotropic Factor and Turbulent Mixing Rate in Rod Bundles Based on Flow Pulsation Phenomenon, Nucl. Tech., Vol. 117, pp. 340-352.

14) Meyer, L. and Rehme, K., 1994, "Large Scale Turbulence Phenomena in Compound Rectangular Channels," Exp. Thermal Fluid Sci., Vol. 8, pp. 286-304.

15) Meyer, L. and Rehme, K., 1995, Periodic Vortices in Flow through Channels with Longitudinal Slots or Fins, Tenth Symp. on Turbulent Shear Flows, P1.

16) Hooper, J. D. and Rehme, K., 1984, Large-Scale Structural Effects in Developed Turbulent Flow through Closely-Spaced Rod Arrays, J. Fluid Mech., Vol. 145, pp. 305-337.

17) Möller, S. V., 1991, On Phenomena of Turbulent Flow through Rod Bundles, Exp. Thermal Fluid Sci., Vol. 4, pp. 25-35.

18) Wu, X. and Trupp, A. C., 1994, Spectral Measurements and Mixing Correlation in Simulated Rod Bundle, Int. J. Heat Mass Transfer, Vol. 37, pp. 1277-1281.

19) Tahir, A. E. E. and Rogers, J. T., 1986, Turbulent Flow Structure in a Closely-Spaced Triangular-Array Rod Bundle, Heat Transfer 1986, Vol. 3, pp. 1035-1040.

20) Meyer, L., 1991, Measurements of Turbulent Velocity and Temperature in a Central Channel of a Heated Rod Bundle, KfK Report 4818, Kernforschungszentrum Karlsruhe, Germany.

21) Krauss, T. and Meyer, L., 1995, Measurements of Turbulent Velocity and Temperature in a Wall Channel of a Heated Rod Bundle, FZKA-Rep. 5582, Forschungszentrum Karlsruhe, FRG.

22) Rehme, K., 1992, The Structure of Turbulence in Rod Bundles and the Implications on Natural Mixing between the Subchannels, Int. J. of Heat Mass Transfer, Vol. 35, pp. 567-581.

23) Kim, S. and Park, G.-C., 1995, Numerical Determination of Lateral Loss Coefficients for Subchannel Analysis in Nuclear Fuel Bundles, Proc. of NUTERH-7, Vol. 4, pp. 2773-2784.

24) Kim, S. and Park, G.-C., 1998, Analysis of Turbulent Mixing in Rod Bundles with an Anisotropic Turbulent Diffusion Model Based on the Flow Pulsation Phenomenon, Nucl. Technol., Vol. 122, pp. 284-294.

25) Lam, C. K. G. and Bremhorst, K., 1981, A Modified Form of the $k-\varepsilon$ Model for Predicting Wall Turbulence, J. Fluids Eng., Vol. 103, pp. 456-460.